
Neural Discovery in Mathematics: Do Machines Dream of Colored Planes?

Konrad Mundinger Max Zimmer Aldo Kiem Christoph Spiegel Sebastian Pokutta

Department for AI in Society, Science, and Technology, Zuse Institute Berlin, Germany

Institute of Mathematics, Technische Universität Berlin, Germany

{mundinger, zimmer, kiem, spiegel, pokutta}@zib.de

Abstract

We demonstrate how neural networks can drive mathematical discovery through a case study of the Hadwiger-Nelson problem, a long-standing open problem from discrete geometry and combinatorics about coloring the plane avoiding monochromatic unit-distance pairs. Using neural networks as approximators, we reformulate this mixed discrete-continuous geometric coloring problem as an optimization task with a probabilistic, differentiable loss function. This enables gradient-based exploration of admissible configurations that most significantly led to the discovery of two novel six-colorings, providing the first improvements in thirty years to the off-diagonal variant of the original problem (Mundinger et al., 2024a). Here, we establish the underlying machine learning approach used to obtain these results and demonstrate its broader applicability through additional results and numerical insights.

1. Introduction

The discovery of mathematical constructions is fundamental to theoretical mathematics, where proving the existence of objects with certain properties can advance our understanding of abstract structures. Traditional computational methods have aided the search for such constructions through exhaustive searches, optimization, and heuristics, while recent advances in Machine Learning (ML) offer new ways to explore mathematical structures and guide intuition. Purely discrete problems can be approached through discrete and combinatorial optimization and purely continuous problems through numerical methods, yet many important theoretical problems involve both discrete and continuous aspects. These mixed discrete-continuous problems have remained particularly challenging for traditional approaches.

The Hadwiger-Nelson (HN) problem perfectly illustrates these challenges: determine the minimum number of colors needed to color the Euclidean plane so that no two

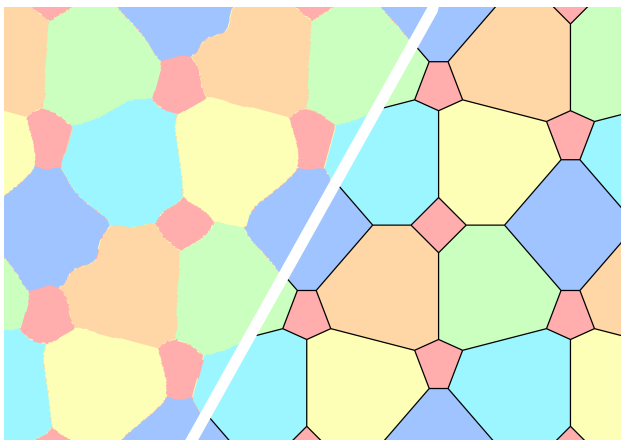


Figure 1: Neural Network output (left) that inspired our formal construction (right) of a novel six-coloring of the plane. Red points avoid all distances between 0.418 and 0.657 while other colors avoid unit distances. The neural network was trained through gradient descent on a continuous and differentiable relaxation of these geometric constraints.

points at unit distance share the same color. This number is often referred to as the *chromatic number of the plane* $\chi(\mathbb{R}^2)$. Despite its simple statement, this problem combines discrete choices (color assignments), continuous geometry (the Euclidean plane), and hard constraints (unit-distance requirements) in a way that has resisted resolution for over seventy years. While SAT solvers and discrete optimization techniques have contributed to finding lower bounds, discovering new colorings has remained challenging.

We present a framework that reformulates this geometric coloring problem as a continuous optimization task by introducing probabilistic colorings and a differentiable loss function. This continuous formulation enables us to use Neural Networks (NNs) as universal function approximators to explore the solution space computationally. The networks return numerical approximations of colorings that are equally capable of representing regular patterns or unexpected, irregular solutions (largely) without any strong built-in assumptions about symmetry or periodicity.

Rather than attempting to obtain proofs that are fully automated end-to-end, our method serves as a tool for mathematical discovery by giving the right intuition about potential constructions. In practice our approach often discovers clearly interpretable patterns and tessellations, generating insights and candidate constructions that still require careful mathematical analysis and formalization. Most notably, this led to the discovery of two novel six-colorings of the plane, see Figure 2 and Figure 12, that provided the first improvement in thirty years to a variant of the original problem where five colors must avoid unit distances while the sixth color avoids a different specified distance, significantly expanding the known range of realizable distances from $[0.415, 0.447]$ to $[0.354, 0.657]$. These constructions have been formally verified and published in a venue specialized in combinatorial geometric problems (Mundinger et al., 2024a). We were also able to extend the range of monochromatic triangles avoidable when coloring the plane, another well-known variant of the HN problem. In this paper, we present the underlying methodology that enabled these discoveries and demonstrate its broader applicability by providing additional numerical insights.

Contributions. Our main contributions are:

1. A continuous optimization framework for geometric coloring problems that uses NNs and probabilistic colorings, enabling gradient-based exploration of solution spaces without strong prior assumptions or discretization of the underlying space.
2. Two novel six-colorings of the plane that provide the first improvement in thirty years to the known range of realizable distances in the off-diagonal HN problem.
3. Numerical evidence motivating the above results and additionally suggesting potential structural properties of solutions to other variants.

Related Literature. Recent years have seen growing interest in applying ML to mathematical discovery, from automated theorem proving to finding novel constructions. We focus on the latter, specifically on approaches that use ML to discover mathematical objects with desired properties. For a broader perspective, we refer to recent surveys by Wang et al. (2023a); Krenn et al. (2022); Williamson (2023).

Several approaches have emerged for using ML in combinatorial discovery. Most closely related to our work, Karalias & Loukas (2020) developed an unsupervised GNN-based framework that uses probabilistic relaxations and differentiable loss functions to solve graph optimization problems. While they focus on purely discrete problems like maximum clique finding, we consider a problem with an inherent continuous structure. Fawzi et al. (2022) solved a discrete optimization problem using a reinforcement learning approach, from which they were able to derive a faster matrix

multiplication algorithm. Similarly, Wagner (2021) studied the ability of a reinforcement-learning approach to construct discrete counterexamples to conjectures in extremal combinatorics. Building on this framework, Roucairol & Cazenave (2022) studied conjectures in spectral graph theory. However, Parczyk et al. (2023) found that this approach was largely outperformed by well-established local searches while studying the Ramsey multiplicity problem. This finding was at least in part supported by the work of Mehrabian et al. (2023). Charton et al. (2024) combine both approaches and propose `PatternBoost`, which trains an NN on the output of a local search and which was also used by Bérczi & Wagner (2024). Taking a markedly different approach, Romera-Paredes et al. (2024) propose `FunSearch`, which uses LLMs to guide greedy search through evolutionary optimization of generated code.

Our approach differs from the approaches used in these results, since we use ML primarily as a tool for mathematical discovery requiring further interpretation and formalization, similar to work of Davies et al. (2021b) on knot invariants invariants that Davies et al. (2021a) later proved formally with significant additional mathematical effort. This approach of using AI to guide mathematical intuition, while still requiring rigorous proof, represents a challenging but underserved direction in AI-assisted mathematics - one that demands expertise in both ML and pure mathematics.

The paradigm of approximating functions by NNs which take coordinates as input is known as *implicit neural representations* (Park et al., 2019; Mescheder et al., 2019; Chen & Zhang, 2019). Our approach adopts this strategy while introducing a loss function that penalizes deviations from desired geometric properties. This connects our method to physics-informed neural networks (Raissi et al., 2019; Cuomo et al., 2022; Wang et al., 2023b), where NNs approximate solutions to differential equations through unsupervised residual minimization. Berzins et al. (2024) recently extended these ideas to geometric constraints.

Finally, our approach fits within the broader *AI4Science* paradigm, where machine learning techniques are revolutionizing scientific discovery in various domains such as protein structure prediction (Jumper et al., 2021) or the earth sciences (Pauls et al., 2024).

2. The Hadwiger-Nelson Problem

First posed in 1950, the HN problem has become one of the most famous open questions in combinatorial geometry and graph theory, with a rich history of partial results and increasingly sophisticated approaches. For a comprehensive treatment of the problem, see Soifer (2009).

Lower bounds for $\chi(\mathbb{R}^2)$ are typically established by constructing unit distance graphs – graphs whose vertices can

be embedded as points in the plane in such a way that edges only connect vertices whose embeddings are a unit distance apart. The Moser spindle establishes that at least four colors are needed (Moser & Moser, 1961) and this bound remained the best known until the breakthrough proof of de Grey (2018) established that $\chi(\mathbb{R}^2) \geq 5$. His construction, originally involving a unit distance graph with 20,425 vertices, sparked intense and largely computational efforts, including through a Polymath project, to simplify and reduce this graph (Heule, 2018; Exoo & Ismailescu, 2020; Parts, 2020a; Polymath, 2021).

Upper bounds on the other hand are commonly established through explicit colorings of the plane. There exists a large number of distinct seven-colorings that avoid monochromatic pairs at unit distance, the first of which used a tiling of congruent regular hexagons and was already discovered in 1950 according to Soifer (2009). This upper bound of $\chi(\mathbb{R}^2) \leq 7$ has remained unchanged since. While computational methods have proven highly successful in establishing lower bounds, there have been surprisingly few systematic computational approaches to constructing new colorings. The only one we are aware of was the use of SAT solvers to color coarsely discretized versions of specific metric spaces as part of the discussions during the Polymath project (Polymath, 2021), highlighting the need for techniques that can explore the continuous solution space more directly.

Given the challenge of closing the gap between the lower and upper bounds of the original problem, several natural variants have been proposed. Solutions to these variants can provide additional insight into the underlying structure and complexity of the original problem.

Variant 1: Almost coloring the plane. A natural question concerns how much of the plane needs to be removed before the remainder can be colored with six colors without monochromatic unit-distance pairs. Pritikin (1998), with a later refinement due to Parts (2020b), established that 99.985% of the plane can be colored with six colors while maintaining this property. This result also effectively bounds the density of a potential counterexample: any unit distance graph requiring seven colors would need to have order at least 6,993, see Lemma 1 by Pritikin (1998) for a proof. The construction uses intersecting pentagonal rods and our NN approach, when applied to the original HN problem with six colors, consistently recovered structures remarkably similar to these pentagonal constructions. Pritikin (1998) also studied the same question for fewer than six colors and we likewise applied our approach in this setting with a modification in the form of a Lagrangian term, see Section 4.1 for a discussion of these results.

Variant 2: Avoiding different distances. Another natural generalization of the problem considers colorings

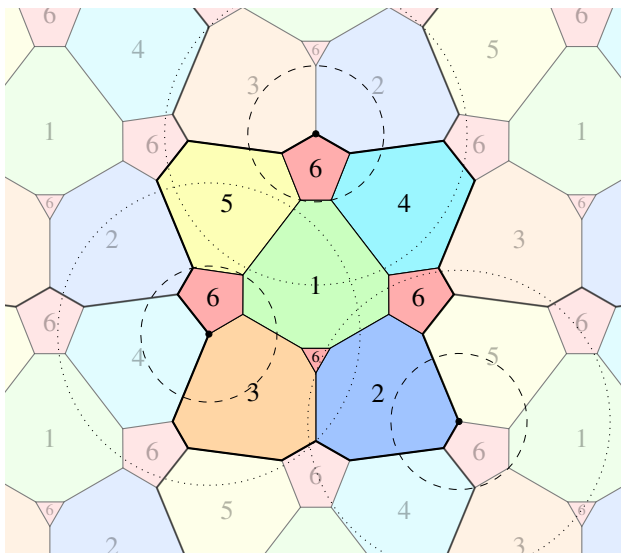


Figure 2: Formalized version of a Neural Network-generated 6-coloring of the plane where no red points appear at distance 0.45 and no other color has monochromatic unit-distance pairs. The dotted circles have unit distance radius while the dashed circle have radius 0.45.

where different colors avoid different distances. More precisely, we say that an k -coloring of the plane has *coloring type* (d_1, \dots, d_k) if color i does not realize distance d_i . This defines a natural ‘off-diagonal’ variant of the original problem, where finding a coloring of type $(1, 1, 1, 1, 1, 1)$ would establish $\chi(\mathbb{R}^2) \leq 6$. Stechkin found a coloring of type $(1, 1, 1, 1, 1/2, 1/2)$ (Raïskii, 1970b) and Woodall (1973) constructed one of type $(1, 1, 1, 1/\sqrt{3}, 1/\sqrt{3}, 1/\sqrt{12})$. Erdős asked for the *polychromatic number of the plane* $\chi_p(\mathbb{R}^2)$ (Soifer, 1992a), that is the smallest number of colors k such that there exist some d_1, \dots, d_k and a coloring of type (d_1, \dots, d_k) . So far no better bounds than $4 \leq \chi_p(\mathbb{R}^2) \leq 6$ are known. Soifer (1992b) found the first six-coloring with a non-unit distance in only one color, having type $(1, 1, 1, 1, 1, 1/\sqrt{5})$. Hoffman & Soifer (1993) later found colorings of type $(1, 1, 1, 1, 1, \sqrt{2} - 1)$. These constructions are part of a family that realizes $(1, 1, 1, 1, 1, d)$ for any $\sqrt{2} - 1 \leq d \leq 1/\sqrt{5}$ (Hoffman & Soifer, 1996; Soifer, 1994b). This led Soifer (1994a) to pose the “still open and extremely difficult” (Nash & Rassias, 2016) problem of determining the continuum of six colorings – that is the set of all d for which a six-coloring of type $(1, 1, 1, 1, 1, d)$ exists.

Using our approach we discovered two novel colorings of the plane that extend the continuum of six colorings (Munding et al., 2024a), providing the first improvement in thirty years. The first coloring is parameterized by d and valid for type $(1, 1, 1, 1, 1, d)$ as long as

$0.354 \leq d \leq 0.553$, see Figure 2. The second coloring is constant and covers the range of $0.418 \leq d \leq 0.657$, see Figure 12. Together they significantly expand the range of distances for which colorings are known to exist. We also explored the polychromatic number computationally but found no way to improve the upper bound, as we will further discuss in Section 4.2.

Variants 3: Coloring n -dimensional space. This variant extends the HN problem to higher dimensions, seeking to determine the chromatic number $\chi(\mathbb{R}^n)$ of n -dimensional space while maintaining the constraint that points at unit distance must receive different colors. A general lower bound of $\chi(\mathbb{R}^n) \geq n+2$ was established by Raiskii (1970a). The three-dimensional case has received particular attention: Nechushtan (2002) proved $\chi(\mathbb{R}^3) \geq 6$ using a graph of approximately 400 vertices, which de Grey (2020) later refined to a 59-vertex construction. Regarding upper bounds, Coulson (2002) famously showed $\chi(\mathbb{R}^3) \leq 15$, a bound that Soifer (2009) conjectures to be tight. Our numerical experiments with 14 colors suggest potential improvements might be possible, as we observe conflicts in only 2% of the points, though these results remain to be formalized. We discuss these findings in more detail in Section 4.3.

Variants 4: Avoiding triangles. Finally, one can ask how many colors are needed to avoid monochromatic triples of points each at unit distances to each other. The answer in this case is actually quite simple: coloring the plane with alternating parallel and half-open stripes of width $\sqrt{3}/2$ using two colors, taking care to include the correct parts of the border of each strip in the color, avoids any monochromatic such triangle. One may again consider a natural off-diagonal version of this problem in which the triples form triangles with prescribed side lengths 1, a , and b for some $0 \leq a, b \leq 1$ satisfying $a + b > 1$. Note that the (degenerate) case $a = 0$ and $b = 1$ corresponds to the original HN problem. A conjecture of Erdős, Graham, Montgomery, Rothschild, Spencer, and Straus (Graham, 2003) states that three colors should always be sufficient, though so far little progress has been made towards that conjecture with some cases, where $a + b$ is close to 1, still requiring seven colors, see Aichholzer & Perz (2019). Currier et al. (2024) recently also proved that any two-coloring contains three-term arithmetic progressions, which can be viewed as a degenerate triangle with $a = b = 0.5$. Using our approach, we were able to extend the previous best bounds in several regions, see Figure 3¹ for an illustration of our current findings, though these bounds may be further improved in future work. See also Section 4.4 for further discussions.

¹Note that Figure 7 in (Aichholzer & Perz, 2019) contained an error that significantly under-reported the size of the four-color region and that has been corrected here.

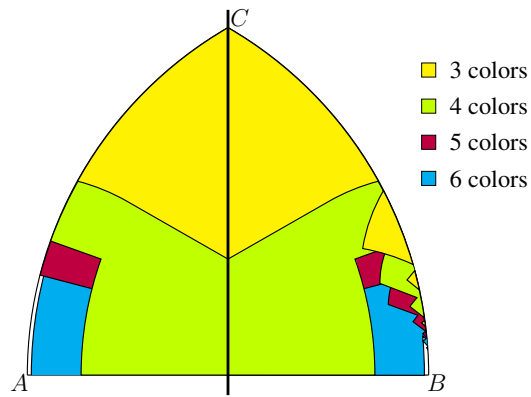


Figure 3: Location of the vertex C of triangles ABC with side AB of length 1 for which a coloring avoiding monochromatic copies of such a triangle is known to exist for between three and six colors. The previously known results due to Aichholzer & Perz (2019) are shown on the left and the results including our improvements on the right.

Many other variants of the HN problem exist, including generalizations to other metric spaces, colorings avoiding arbitrary unit-distance graphs, or colorings avoiding several distinct differences in each color. Our framework should be largely applicable to these variants with minimal modifications, providing a systematic tool for exploring potential constructions.

3. Methodology

In this section we develop the formulation of the HN problem as a continuous optimization problem using probabilistic colorings. The original problem asks whether there exists a function $g: \mathbb{R}^2 \rightarrow \{1, \dots, c\}$ such that

$$g(x) \neq g(y) \quad \forall x, y \in \mathbb{R}^2 \text{ with } \|x - y\|_2 = 1. \quad (1)$$

We relax the constraints by replacing the discrete color assignment with a probabilistic one. Instead of assigning a fixed color to each point, we assign a probability distribution over the c colors, represented by a mapping $p: \mathbb{R}^2 \rightarrow \Delta_c$, where Δ_c is the c -dimensional probability simplex. The inner product $p(x)^T p(y)$ then naturally captures the probability that points x and y receive the same color when independently sampling from their respective distributions.

Given such a probabilistic coloring p , we define a loss function measuring the violation of the unit distance constraint in $[-R, R]^2$ through

$$\mathcal{L}_R(p) = \int_{[-R, R]^2} \int_{\partial B_1(x)} p(x)^T p(y) d\nu(y) d\mu(x), \quad (2)$$

where $\partial B_r(x) = \{y \in \mathbb{R}^2 \mid \|x - y\| = r\}$ denotes the euclidean sphere of radius r around x and $\nu = \mathcal{U}(\partial B_1(x))$

as well as $\mu = \mathcal{U}([-R, R]^2)$ are uniform distributions over $\partial B_1(x)$ and $[-R, R]^2$, respectively. The inner integral represents the probability of a conflict between a fixed point x and a randomly sampled point y at unit distance from it, while the outer integral averages this over all points in $[-R, R]^2$. While we are ultimately interested in this loss as R tends to infinity, in practice we study it for some fixed (small) value of R and aim to solve

$$\arg \min_p \mathcal{L}_R(p). \quad (3)$$

A coloring of a finite box $[-R, R]^2$ does not necessarily extend to a valid coloring of the entire plane \mathbb{R}^2 . However, our objective is to find patterns within this box that can be periodically extended across the plane. Clearly, any valid discrete coloring g of the plane can be converted to a probabilistic coloring p through one-hot-encoding, yielding $\mathcal{L}_R(p) = 0$ for all $R > 0$. In the other direction, we have the following simple result.

Proposition 3.1. *If $R > 0$ and p is a probabilistic coloring with $\mathcal{L}_R(p) = 0$, then the coloring given by $g(x) = \arg \max (p(x))$ satisfies Equation (1) for almost all pairs $\{(x, y) \in [-R, R]^2 \times \mathbb{R}^2 \mid \|x - y\| = 1\}$.*

Proof. Let $X \subseteq [-R, R]^2$ denote the set of points x for which the inner integral $\int_{\partial B_1(x)} p(x)^T p(y) dy$ is non-zero and for any given $x \in [-R, R]^2$ let $Y(x) \subseteq \partial B_1(x)$ denote the set of points y for which the support of $p(y)$ is not disjoint from $p(x)$, i.e., the points y with $p(x)^T p(y) > 0$. By basic properties of the Lebesgue measure and since $p(x)^T p(y)$ in the definition of $\mathcal{L}_R(g)$ is non-negative as a dot product of probability vectors, X has measure zero in $[-R, R]^2$ and so does $Y(x)$ in $\partial B_1(x)$ for any $x \in [-R, R]^2 \setminus X$. It follows that $\{(x, y) \mid x \in X, y \in \partial B_1(x)\} \cup \{(x, y) \mid x \in [-R, R]^2 \setminus X, y \in Y(x)\}$, likewise has measure zero with respect to the uniform distribution over $\{(x, y) \in [-R, R]^2 \times \mathbb{R}^2 \mid \|x - y\| = 1\}$. \square

The minimization of Equation (2) over probabilistic colorings therefore provides a path to finding colorings for the original HN problem through Proposition 3.1, assuming a suitably parameterized family of functions that ideally can approximate arbitrary colorings.

3.1. Parameterizing the space of probabilistic colorings

We approximate probabilistic colorings p through NNs p_θ of fixed architecture and size with trainable parameters θ , turning Equation (3) into the finite-dimensional optimization problem $\arg \min_\theta \mathcal{L}_R(p_\theta)$. By virtue of the universal approximation property (Cybenko, 1989) and their inherent spectral bias towards low-frequency functions (Rahaman et al., 2019), NNs provide both the expressiveness needed to capture complex spatial patterns and a natural tendency

towards structured, interpretable solutions. We employ a standard multilayer perceptron that encodes geometric structure through its loss function, making this a geometric learning approach despite its simple architecture. Following best practices for implicit neural representations (Sitzmann et al., 2020), we implement p_θ as a SIREN architecture with sine activation functions. The networks we used consisted of two to four hidden linear layers with 64 to 256 neurons each, directly mapping coordinates to color distributions through a softmax activation after the final layer.

3.2. Batched gradient descent

To minimize the loss function, we employ gradient descent on the NN parameters θ . The main challenge lies in approximating $\nabla_\theta \mathcal{L}_R(p_\theta)$, which involves nested integrals that we approximate through Monte Carlo sampling. Specifically, we sample n center points $x_i \sim \mathcal{U}([-R, R]^2)$ and, for each center x_i , sample m points $y_{ij} \sim \mathcal{U}(\partial B_1(x_i))$. Using automatic differentiation, we obtain the estimate

$$\nabla_\theta \mathcal{L}_R(p_\theta) \approx \nabla_\theta \left[\frac{1}{nm} \sum_{i=1}^n \sum_{j=1}^m p_\theta(x_i)^T p_\theta(y_{ij}) \right]. \quad (4)$$

3.3. Addressing the four variants

We demonstrate how the formulation in Equation (2) can be adapted to the four variants described in Section 2, including necessary adjustments to the NN and sampling procedures already described.

Variant 1: Almost coloring the plane. To formalize the idea of an *almost coloring*, we introduce an additional color, in which no conflicts are penalized. We extend the codomain of p_θ to Δ_{c+1} , with the last entry corresponding to the additional color. Formally, we then want to solve the constrained optimization problem

$$\begin{aligned} & \arg \min_{p_\theta} \mathcal{L}_R(p_\theta^c) \\ \text{s.t.} & \int_{[-R, R]^2} p_\theta(x)_{c+1} d\mu(x) \leq \delta \end{aligned}$$

for some pre-determined $\delta > 0$, where p_θ^c refers to the first c components of p_θ . More precisely, we want to determine the minimum δ for which the answer to this problem is zero. In practice, we solve the Lagrangian relaxation

$$\mathcal{L}_R^\lambda(p_\theta) = \mathcal{L}_R(p_\theta^c) + \lambda \int_{[-R, R]^2} p_\theta(x)_{c+1} d\mu(x). \quad (5)$$

While in theory there exists a corresponding λ for each δ , we simply treat λ as a hyperparameter controlling the trade-off between using the additional color and maintaining valid colorings.

Variation 2: Avoiding different distances. If the desired coloring is of type (d_1, \dots, d_c) , we modify the loss formulation to

$$\sum_{k=1}^c \int_{[-R, R]^2} \int_{\partial B_{d_k}(x)} p_\theta(x)_k p_\theta(y)_k d\nu_k(y) d\mu(x), \quad (6)$$

with $\mu = \mathcal{U}([-R, R]^2)$ and $\nu_k = \mathcal{U}(B_{d_k}(x))$, i.e., we now need to choose the points y from the sphere $\partial B_{d_k}(x)$ of radius d_k around x for each color k . Minimizing the loss function finds probabilistic colorings that avoid distance d_k for color k . Note that we recover Equation (2) for $d_1 = \dots = d_c = 1$.

This model can also be extended to handle sets or ranges of distances for some or all colors. To achieve this, we redefine the domain of the candidate functions g to include the current distance. Given distance ranges $[d_k^{\min}, d_k^{\max}]$ for each color k for example, we define

$$p : \mathbb{R}^2 \times \prod_{k=1}^c [d_k^{\min}, d_k^{\max}] \rightarrow \Delta_c. \quad (7)$$

By integrating Equation (6) over this expanded domain, we average the loss across all distances within the specified range for each color by sampling points on c circles, corresponding to the distances d_k , $k = 1, \dots, c$. Note that this increases the effective batch size from nm to $nm c$. This approach allows exploration of a larger part of the solution space instead of just a single type.

Variation 3: Coloring n -dimensional space. To extend to higher dimensions, it suffices to integrate over \mathbb{R}^n and letting $\partial B_1(x)$ represent the sphere in the appropriate space. We are particularly interested in the three-dimensional case. Apart from adapting the input dimension of g_θ as well as sampling in the higher dimensional space, this case is analogous to the two dimensional cases.

Variation 4: Avoiding triangles. If we want to avoid monochromatic triangles with side lengths 1, a and b such that $a+b > 1$, we simply replace the integrand $p_\theta(x)_k p_\theta(y)_k$ in Equation (2) with

$$\sum_{k=1}^c p_\theta(x)_k p_\theta(y)_k (p_\theta(z_1)_k + p_\theta(z_2)_k) / 2 \quad (8)$$

where z_1 and z_2 are the two candidates for the the point z such that x , y , and z form a triangle with $\|x - y\| = 1$, $\|x - z\| = a$ and $\|y - z\| = b$.

In this variant we sample center points $x \in [-R, R]^2$ and proximity points y on the unit circle as before. We then obtain the two candidates z_1 and z_2 for the third point of the triangle by calculating the intersection points of the

circles of radius a and b around x and y , respectively. As in Variation 2, the domain of the function p can be extended to $\mathbb{R}^2 \times [a_{\min}, a_{\max}] \times [b_{\min}, b_{\max}]$ to allow for continuous ranges of a and b within one network and we integrate the loss over the intervals $[a_{\min}, a_{\max}]$ and $[b_{\min}, b_{\max}]$.

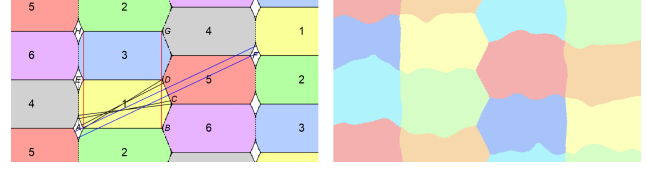


Figure 4: The almost-coloring due to Pritikin (1998) and Parts (2020b) (left) and the coloring suggest by our approach (right). The wavy lines are caused by the inherent degrees of freedom present in many colorings.

4. Experimental results

In this section we present our numerical results for the original HN problem and its four variants. We implemented our approach in PyTorch, updating the parameters using the Adam optimizer (Kingma, 2014) with a learning rate schedule linearly decaying (Li et al., 2019) from an initial value of between 10^{-3} and 10^{-4} . We typically used between 16,384 and 65,536 training steps, sampling 1,024 to 4,096 points for x and 1 to 32 points for y on the circle(s) around x during each step, resulting in 10^6 to 10^{10} total samples during training. A single such run takes between five and 20 minutes on an NVIDIA V100 GPU, though adequate results can be achieved in under 20 minutes on a standard laptop CPU with reduced batch sizes and a decreased number of steps. Due to the heuristic nature of our approach and the need to tune hyperparameters, we did however perform hundreds to thousands of runs for each variant, particularly when exploring parameter spaces in the off-diagonal and triangle variants.

Our initial experiments focused on six-color solutions in the classical setting. The method consistently recovered patterns resembling Pritikin’s construction, providing early validation of our approach, see Figure 4. However, these results also revealed that neural networks often introduce irregularities such as wavy lines, reflecting inherent freedoms in the solution space. This becomes even more pronounced for seven colors, see Figure 9 in the appendix. These findings highlight that our method can successfully discover valid colorings, but formalizing the discovered patterns into rigorous mathematical constructions may still require substantial additional effort. Additionally, the method’s inability to suggest valid colorings with fewer than seven colors provides additional numerical evidence that the chromatic number of the plane may in fact be seven.

4.1. Variant 1: Almost coloring the plane

Applying the Lagrangian-modified loss function described in Section 3.3 to six colors, we achieved conflict rates of around 0.05%, slightly higher than those reported by Parts (2020b). The optimization process proved sensitive to the Lagrangian term λ , but consistently recovered known constructions once a good range (typically between 10^{-3} and 10^{-2}) was found. We report results for $k = 2, \dots, 5$ colors in Table 1. The discovered patterns for two to four colors closely match known constructions, see Figure 10 in the appendix. The five-color case exhibits slightly different patterns from those described by (Parts, 2020b), though these have not yet been formalized and it is unclear if they would provide any improvements.

Table 1: Comparison of our results to the best known results for the almost coloring of the plane. We report the fraction of points that need to be removed to color the remainder while avoiding unit distance. Our results represent the best value of 60 runs and are only numerical approximations within a box of size $[-3, 3]^2$. Due to the similarity to known constructions, we do not expect that the suggested improvements for two and three colors can in fact be realized by a formal coloring.

# colors	2	3	4	5	6
Best known	54.1271%	31.1905%	8.2541%	4.0060%	0.0143%
Our numerics	51.03%	29.38%	8.68%	4.01%	0.03%

4.2. Variant 2: Avoiding different distances

We report the numerical results on colorings of type (d_1, \dots, d_6) with a particular focus on the cases $d_i = 1$ for either $i \in \{1, \dots, 5\}$ or $i \in \{1, \dots, 4\}$.

Colorings of type $(1, 1, 1, 1, 1, d)$ Following Section 3, we included the free distance d in the domain of the coloring function, exploring the interval $[0.2, 2.2]$. This approach not only allows optimization over a continuous range of distances but also reveals smooth transitions between colorings, see Figure 13 in the appendix, which proved crucial in identifying a broader family of valid solutions. Figure 5 shows the conflict rates as a function of d for sixteen individual runs and their pointwise minimum. While previous work established valid colorings for $d \in [\sqrt{2} - 1, 1/\sqrt{5}]$ (orange dashed lines), our constructions extend this range to $[0.354, 0.657]$ (blue dashed lines). Additional regions of interest appear at $d \approx 1$, corresponding to the vanilla HN problem and $d \approx 1.6$, where conflict rates fall below 1%.

Colorings of type $(1, 1, 1, 1, d_1, d_2)$ Analogously, we treated the last two colors as free distances and augmented the domain of the NNs by them. The resulting colorings remain continuous in both d_1 and d_2 . As shown in Figure 6,

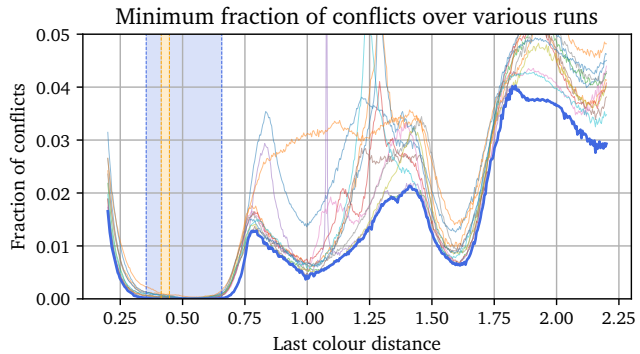


Figure 5: Fraction of conflicting points versus the free distance d in $(1, 1, 1, 1, 1, d)$ colorings. The thick blue line shows the minimum over multiple runs (thin lines). Orange and blue shaded regions indicate the previously known and our extended ranges of valid colorings, respectively.

we found three regions of minimal conflicts: two symmetric regions near $(d_1, 1)$ and $(1, d_2)$ with $d_1, d_2 \approx 0.5$, recovering our earlier $(1, 1, 1, 1, 1, d)$ colorings, and an additional region near $(0.5, 0.5)$ corresponding to a construction similar to Stechkin’s, see Figure 13.

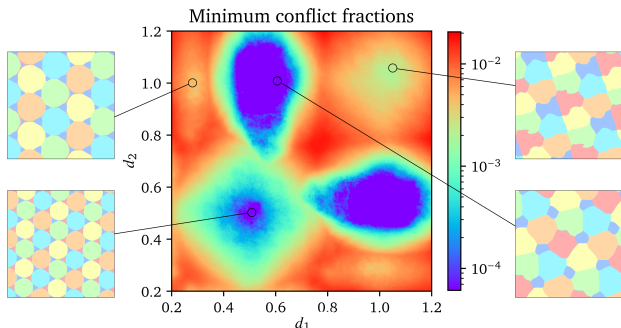


Figure 6: The fraction of conflicts in $(1, 1, 1, 1, d_1, d_2)$ colorings as a function of d_1 and d_2 (center, showing minimum over sixteen networks). Three regions of minimal conflicts emerge: symmetric regions near $(d_1, 1)$ and $(1, d_2)$ with $d_1, d_2 \approx 0.5$, and one near $(0.5, 0.5)$. Sample colorings from these regions are shown in the surrounding plots.

Polychromatic Number We investigated potential five-color solutions of type (d_1, \dots, d_5) by including the distances in the domain of the NN and determining the best candidates for such a type after training using first- and second-order methods. Our result achieved a minimal conflict rate of 4.9% with distances $d_1 = 1$, $d_2 \approx d_3 \approx 1$, and $d_4 \approx d_5 \approx 0.56$, see Figure 7. Despite extensive optimization, our inability to find a conflict-free five-color solution provides additional evidence that the polychromatic number may indeed be six. More details are provided in Appendix C.

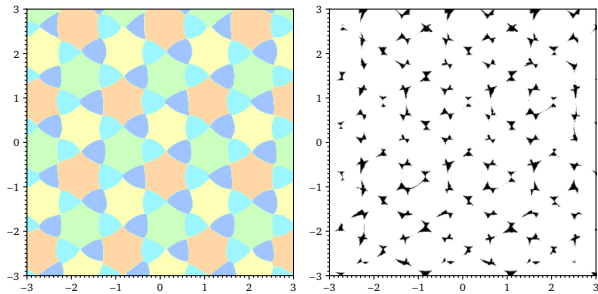


Figure 7: The best five-coloring with $d_1 = 1$, $d_2 \approx d_3 \approx 1$ and $d_4 \approx d_5 \approx 0.56$ and approximately 5% of conflicts in a box of size $[-3, 3]^2$.

4.3. Variant 3: Coloring n -dimensional space

Our method successfully found conflict-free 15-color solutions, consistent with the bound established by Coulson (2002). In attempting to improve this bound, our best 14-color solution achieved a conflict rate of approximately 2% when evaluated in a $[-3, 3]^3$ box. While a simple discretization could potentially yield an almost-coloring requiring removal of only 1-2% of space, we are currently still in the process of deriving a more mathematically satisfying formalization. This remains challenging due to increased complexity of three-dimensional patterns, which makes both visualization and interpretation significantly more difficult than in the planar case. More details are provided in Appendix D.

4.4. Variant 4: Avoiding triangles

We applied our approach to study triangles with sides of length 1, a , and b where $a + b > 1$. For four and five colors, our neural networks consistently discovered constructions based on stripes and hexagonal tessellations, similar to those used by Aichholzer & Perz (2019). However, the numerical results suggested that alternative scalings of these basic patterns could yield improvements beyond those previously known, see the suggested patterns in Figure 8. We were able to formalize some of those based on stripes, obtaining several new bounds that expand the regions where three to five colors suffice, as already shown previously in Figure 3. This significantly reduces the area of the parameter space still requiring seven colors, though further improvements seem possible.

Beyond further resolving the parameter space with respect to the number of required colors both numerically (Figure 8) as well as via formalized patterns (Figure 3), the numerical results also provide evidence against Graham’s conjecture (Graham, 2003) that three colors should always suffice: our experiments consistently required more colors as one side of the triangle became shorter while the other became closer

to unit length, suggesting these cases (which more closely resemble the original HN problem) may be fundamentally more challenging.

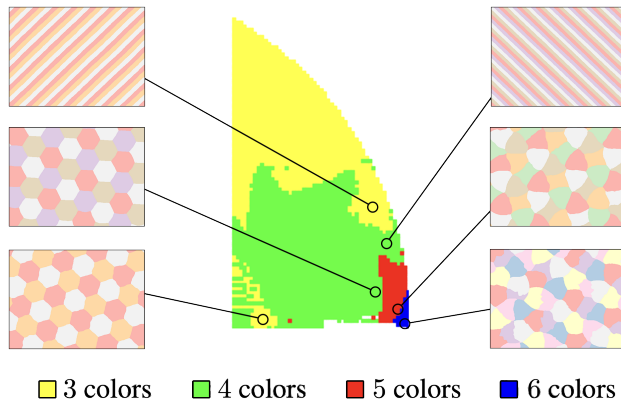


Figure 8: Numerical results showing the achievable color bounds when avoiding monochromatic triangles, together with a selection of found colorings. We trained thousands of networks on different sub-areas of the above region and say that a point can be achieved with three, four, five, or six colors if the top 3% of runs for that point reported that less than 0.1% of sampled triangles were monochromatic in the argmax coloring derived from the trained NNs.

5. Discussion

Our framework provides a novel approach to exploring mathematical structures through continuous optimization, leading to several concrete improvements to long-standing open problems. Beyond just being applicable to variants of the HN problem, we believe that it naturally extends to other problems in discrete geometry and extremal combinatorics. For instance, graph-theoretic problems involving discrete structures can often be reformulated through graph limits, where the objective becomes optimizing over continuous maps $[0, 1]^2 \rightarrow [0, 1]$. Our approach of using neural networks as universal function approximators combined with suitable loss functions could be directly applied in this setting. The framework could also potentially be extended to handle non-differentiable losses through the introduction of auxiliary ‘critic’ or ‘value’ networks that learn to approximate these losses, similar to techniques used in adversarial and reinforcement learning. More broadly, this work demonstrates how continuous relaxations and gradient-based optimization can bridge the gap between machine learning and mathematical discovery, potentially opening new paths to approaching long-standing open problems in discrete mathematics.

Acknowledgements

Research reported in this paper was partially supported through the AI4Forest project, which is funded by the German Federal Ministry of Education and Research (BMBF; grant number 01IS23025A) and the Deutsche Forschungsgemeinschaft (DFG) through the DFG Cluster of Excellence MATH+ (grant number EXC-2046/1, project ID 390685689) as well as Sonderforschungsbereich (SFB) Transregio 154 (grant number 239904186). We also thank Sagdeev Arsenii for suggesting the triangle variant of the HN problem.

References

- Aichholzer, O. and Perz, D. Triangles in the colored euclidean plane. In *35th European Workshop on Computational Geometry (EuroCG 2019)*, 2019.
- Barthe, F., Guédon, O., Mendelson, S., and Naor, A. A probabilistic approach to the geometry of the lpn-ball. *The Annals of Probability*, 33(2):480–513, March 2005. ISSN 0091-1798, 2168-894X. doi: 10.1214/009117904000000874.
- Bérczi, G. and Wagner, A. Z. A note on small percolating sets on hypercubes via generative AI. *arXiv preprint arXiv:2411.19734*, 2024.
- Berzins, A., Radler, A., Volkmann, E., Sanokowski, S., Hochreiter, S., and Brandstetter, J. Geometry-informed neural networks. *arXiv preprint arXiv:2402.14009*, (arXiv:2402.14009), October 2024. doi: 10.48550/arXiv.2402.14009. URL <http://arxiv.org/abs/2402.14009>. arXiv:2402.14009 [cs].
- Charton, F., Ellenberg, J. S., Wagner, A. Z., and Williamson, G. PatternBoost: Constructions in mathematics with a little help from AI. *arXiv preprint arXiv:2411.00566*, 2024.
- Chen, Z. and Zhang, H. Learning implicit fields for generative shape modeling. *2019 IEEE/CVF Conference on Computer Vision and Pattern Recognition (CVPR)*, pp. 5932–5941, June 2019. doi: 10.1109/CVPR.2019.00609.
- Coulson, D. A 15-colouring of 3-space omitting distance one. *Discrete mathematics*, 256(1-2):83–90, 2002.
- Cuomo, S., Cola, V. S. d., Giampaolo, F., Rozza, G., Raissi, M., and Piccialli, F. Scientific machine learning through physics-informed neural networks: Where we are and what’s next. (arXiv:2201.05624), June 2022. doi: 10.48550/arXiv.2201.05624. URL <http://arxiv.org/abs/2201.05624>. arXiv:2201.05624 [cs].
- Currier, G., Moore, K., and Yip, C. H. Any two-coloring of the plane contains monochromatic 3-term arithmetic progressions. *Combinatorica*, 44(6):1367–1380, December 2024. ISSN 1439-6912. doi: 10.1007/s00493-024-00122-2.
- Cybenko, G. Approximation by superpositions of a sigmoidal function. *Mathematics of control, signals and systems*, 2(4):303–314, 1989.
- Davies, A., Juhász, A., Lackenby, M., and Tomasev, N. The signature and cusp geometry of hyperbolic knots. *arXiv preprint arXiv:2111.15323*, 2021a.
- Davies, A., Veličković, P., Buesing, L., Blackwell, S., Zheng, D., Tomašev, N., Tanburn, R., Battaglia, P., Blundell, C., Juhász, A., et al. Advancing mathematics by guiding human intuition with AI. *Nature*, 600(7887): 70–74, 2021b.
- de Grey, A. D. The chromatic number of the plane is at least 5. *Geombinatorics Quarterly*, XXVIII(1):18–31, 2018.
- de Grey, A. D. N. J. A small 6-chromatic unit-distance graph in \mathbb{R}^3 . *Geombinatorics Quarterly*, XXX(1):5–13, 2020.
- Exoo, G. and Ismailescu, D. The chromatic number of the plane is at least 5: a new proof. *Discrete & Computational Geometry*, 64(1):216–226, 2020.
- Fawzi, A., Balog, M., Huang, A., Hubert, T., Romera-Paredes, B., Barekatin, M., Novikov, A., R Ruiz, F. J., Schrittwieser, J., Swirszcz, G., et al. Discovering faster matrix multiplication algorithms with reinforcement learning. *Nature*, 610(7930):47–53, 2022.
- Graham, R. Problem 58: Monochromatic triangles. The Open Problems Project (TOPP), 2003. Available at <http://cs.smith.edu/~orourke/TOPP/P58.html#Problem.58>.
- Heule, M. J. Computing small unit-distance graphs with chromatic number 5. *Geombinatorics Quarterly*, XXVIII(1):32–50, 2018.
- Hoffman, I. and Soifer, A. Almost chromatic number of the plane. *Geombinatorics*, 3(2):38–40, 1993.
- Hoffman, I. and Soifer, A. Another six-coloring of the plane. *Discrete Mathematics*, 150(1-3):427–429, 1996.
- Jumper, J., Evans, R., Pritzel, A., Green, T., Figurnov, M., Ronneberger, O., Tunyasuvunakool, K., Bates, R., Žídek, A., Potapenko, A., Bridgland, A., Meyer, C., Kohl, S. A. A., Ballard, A. J., Cowie, A., Romera-Paredes, B., Nikolov, S., Jain, R., Adler, J., Back, T., Petersen, S., Reiman, D., Clancy, E., Zielinski, M., Steinegger, M., Pacholska, M., Berghammer, T., Bodenstern, S., Silver, D., Vinyals, O., Senior, A. W., Kavukcuoglu,

- K., Kohli, P., and Hassabis, D. Highly accurate protein structure prediction with alphafold. *Nature*, 596 (7873):583–589, August 2021. ISSN 1476-4687. doi: 10.1038/s41586-021-03819-2.
- Karalias, N. and Loukas, A. Erdős goes neural: an unsupervised learning framework for combinatorial optimization on graphs. *Advances in Neural Information Processing Systems*, 33:6659–6672, 2020.
- Kingma, D. P. Adam: A method for stochastic optimization. *arXiv preprint arXiv:1412.6980*, 2014.
- Kovachki, N. B., Lanthaler, S., and Stuart, A. M. Operator learning: Algorithms and analysis. (arXiv:2402.15715), February 2024. doi: 10.48550/arXiv.2402.15715. URL <http://arxiv.org/abs/2402.15715>. arXiv:2402.15715 [cs].
- Krenn, M., Pollice, R., Guo, S. Y., Aldeghi, M., Cervera-Lierta, A., Friederich, P., dos Passos Gomes, G., Häse, F., Jinich, A., Nigam, A., et al. On scientific understanding with artificial intelligence. *Nature Reviews Physics*, 4 (12):761–769, 2022.
- Li, M., Yumer, E., and Ramanan, D. Budgeted training: Rethinking deep neural network training under resource constraints. *arXiv preprint arXiv:1905.04753*, 2019.
- Lu, L., Jin, P., Pang, G., Zhang, Z., and Karniadakis, G. E. Learning nonlinear operators via deepnet based on the universal approximation theorem of operators. *Nature Machine Intelligence*, 3(3):218–229, March 2021. ISSN 2522-5839. doi: 10.1038/s42256-021-00302-5.
- Mehrabian, A., Anand, A., Kim, H., Sonnerat, N., Balog, M., Comanici, G., Berariu, T., Lee, A., Ruoss, A., Bulanova, A., et al. Finding increasingly large extremal graphs with AlphaZero and tabu search. *arXiv preprint arXiv:2311.03583*, 2023.
- Mescheder, L., Oechsle, M., Niemeyer, M., Nowozin, S., and Geiger, A. Occupancy networks: Learning 3d reconstruction in function space. In *2019 IEEE/CVF Conference on Computer Vision and Pattern Recognition (CVPR)*, pp. 4455–4465, June 2019. doi: 10.1109/CVPR.2019.00459. URL <https://ieeexplore.ieee.org/document/8953655>.
- Moser, L. and Moser, W. Solution to problem 10. *Canad. Math. Bull.*, 4:187–189, 1961.
- Mundinger, K., Pokutta, S., Spiegel, C., and Zimmer, M. Extending the continuum of six-colorings. *Geombinatorics Quarterly*, XXXIV, 2024a. URL <https://geombina.uccs.edu/past-issues/volume-xxxiv>.
- Mundinger, K., Zimmer, M., and Pokutta, S. Neural parameter regression for explicit representations of pde solution operators, 2024b.
- Nash, J. F. and Rassias, M. T. *Open problems in mathematics*. Springer, 2016.
- Nechushtan, O. On the space chromatic number. *Discrete mathematics*, 256(1-2):499–507, 2002.
- Parczyk, O., Pokutta, S., Spiegel, C., and Szabó, T. Fully computer-assisted proofs in extremal combinatorics. In *Proceedings of the AAAI Conference on Artificial Intelligence*, volume 37, pp. 12482–12490, 2023.
- Park, J. J., Florence, P., Straub, J., Newcombe, R., and Lovegrove, S. DeepSDF: Learning continuous signed distance functions for shape representation. In *2019 IEEE/CVF Conference on Computer Vision and Pattern Recognition (CVPR)*, pp. 165–174, June 2019. doi: 10.1109/CVPR.2019.00025. URL <https://ieeexplore.ieee.org/document/8954065>.
- Parts, J. Graph minimization, focusing on the example of 5-chromatic unit-distance graphs in the plane. *arXiv preprint arXiv:2010.12665*, 2020a.
- Parts, J. What percent of the plane can be properly 5- and 6-colored? *arXiv preprint arXiv:2010.12668*, 2020b.
- Pauls, J., Zimmer, M., Kelly, U. M., Schwartz, M., Saatchi, S., Ciais, P., Pokutta, S., Brandt, M., and Gieseke, F. Estimating Canopy Height at Scale. *Proceedings of ICML*, 5 2024.
- Polymath, D. On the chromatic number of circular disks and infinite strips in the plane. *Geombinatorics Quarterly*, XXX(4):190–201, 2021.
- Pritikin, D. All unit-distance graphs of order 6197 are 6-colorable. *Journal of Combinatorial Theory, Series B*, 73 (2):159–163, 1998.
- Rahaman, N., Baratin, A., Arpit, D., Draxler, F., Lin, M., Hamprecht, F. A., Bengio, Y., and Courville, A. On the spectral bias of neural networks. (arXiv:1806.08734), May 2019. doi: 10.48550/arXiv.1806.08734. URL <http://arxiv.org/abs/1806.08734>. arXiv:1806.08734 [stat].
- Raiskii, D. E. Realization of all distances in a decomposition of the space \mathbb{R}^n into $n+1$ parts. *Mathematical notes of the Academy of Sciences of the USSR*, 7(3):194–196, 1970a. doi: 10.1007/BF01093113. URL <https://doi.org/10.1007/BF01093113>.
- Raiskii, D. E. Realization of all distances in a decomposition of the space \mathbb{R}^n into $n+1$ parts. *Mathematical notes of the Academy of Sciences of the USSR*, 7:194–196, 1970b.

- Raissi, M., Perdikaris, P., and Karniadakis, G. E. Physics-informed neural networks: A deep learning framework for solving forward and inverse problems involving nonlinear partial differential equations. *Journal of Computational Physics*, 378:686–707, February 2019. ISSN 0021-9991. doi: 10.1016/j.jcp.2018.10.045.
- Romera-Paredes, B., Barekatin, M., Novikov, A., Balog, M., Kumar, M. P., Dupont, E., Ruiz, F. J., Ellenberg, J. S., Wang, P., Fawzi, O., et al. Mathematical discoveries from program search with large language models. *Nature*, 625 (7995):468–475, 2024.
- Roucairol, M. and Cazenave, T. Refutation of spectral graph theory conjectures with Monte Carlo search. In *International Computing and Combinatorics Conference*, pp. 162–176. Springer, 2022.
- Sitzmann, V., Martel, J., Bergman, A., Lindell, D., and Wetzstein, G. Implicit neural representations with periodic activation functions. *Advances in neural information processing systems*, 33:7462–7473, 2020.
- Soifer, A. Relatives of chromatic number of the plane I. *Geombinatorics*, 1(4):13–17, 1992a.
- Soifer, A. A six-coloring of the plane. *Journal of Combinatorial Theory, Series A*, 61(2):292–294, 1992b.
- Soifer, A. Six-realizable set X_6 . *Geombinatorics*, III(4): 140–145, 1994a.
- Soifer, A. An infinite class of six-colorings of the plane. *Congressus Numerantium*, pp. 83–86, 1994b.
- Soifer, A. *The mathematical coloring book: Mathematics of coloring and the colorful life of its creators*. Springer, 2009.
- Wagner, A. Z. Constructions in combinatorics via neural networks. *arXiv preprint arXiv:2104.14516*, 2021.
- Wang, H., Fu, T., Du, Y., Gao, W., Huang, K., Liu, Z., Chandak, P., Liu, S., Van Katwyk, P., Deac, A., et al. Scientific discovery in the age of artificial intelligence. *Nature*, 620(7972):47–60, 2023a.
- Wang, S., Wang, H., and Perdikaris, P. Learning the solution operator of parametric partial differential equations with physics-informed deepoanets. *Science Advances*, 7(40): eabi8605, September 2021. doi: 10.1126/sciadv.abi8605.
- Wang, S., Sankaran, S., Wang, H., and Perdikaris, P. An expert’s guide to training physics-informed neural networks. (arXiv:2308.08468), August 2023b. doi: 10.48550/arXiv.2308.08468. URL <http://arxiv.org/abs/2308.08468>. arXiv:2308.08468 [physics].
- Williamson, G. Is deep learning a useful tool for the pure mathematician? *arXiv preprint arXiv:2304.12602*, 2023.
- Woodall, D. R. Distances realized by sets covering the plane. *Journal of Combinatorial Theory, Series A*, 14(2): 187–200, 1973.

A. Coloring the plane with seven colors

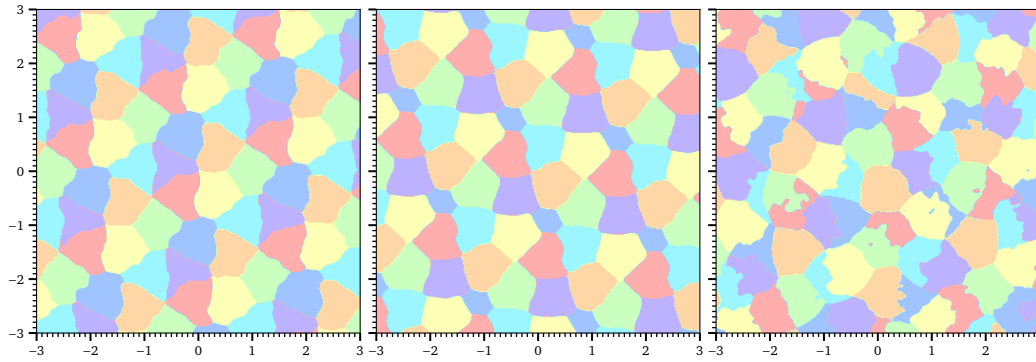


Figure 9: Colorings found for the HN problem with seven colors. Left and middle: Rather structured colorings. Right: Less structured coloring.

B. Details on variant 1: Almost coloring the plane

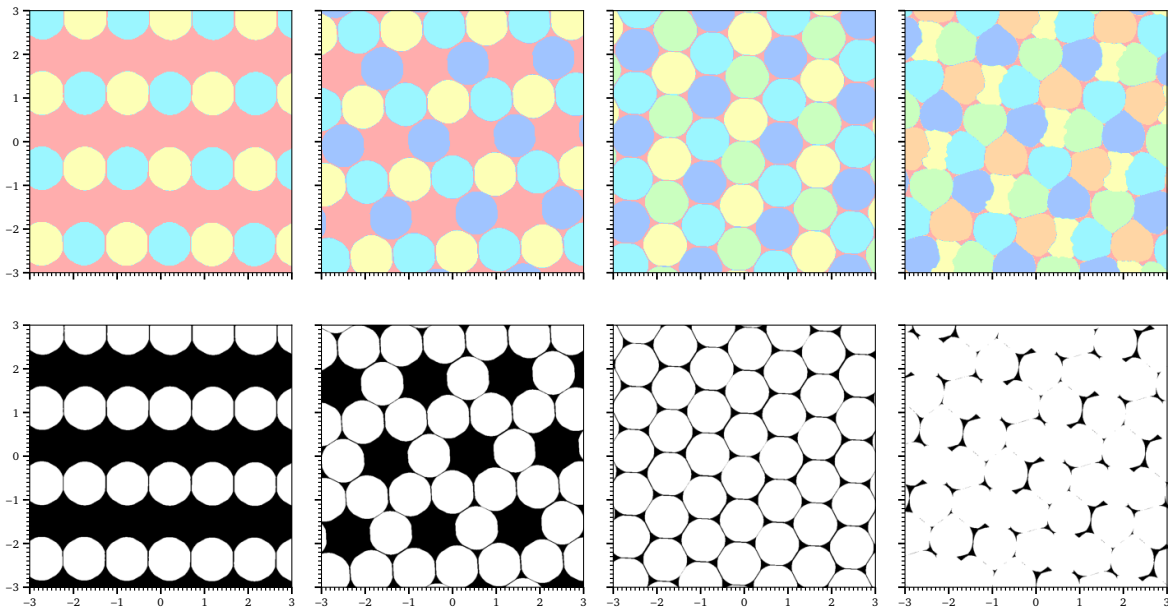


Figure 10: Almost-colorings for two, three, four, and five colors (from left to right). Top row shows the colorings, bottom row shows the points needed to be removed to avoid unit distance conflicts.

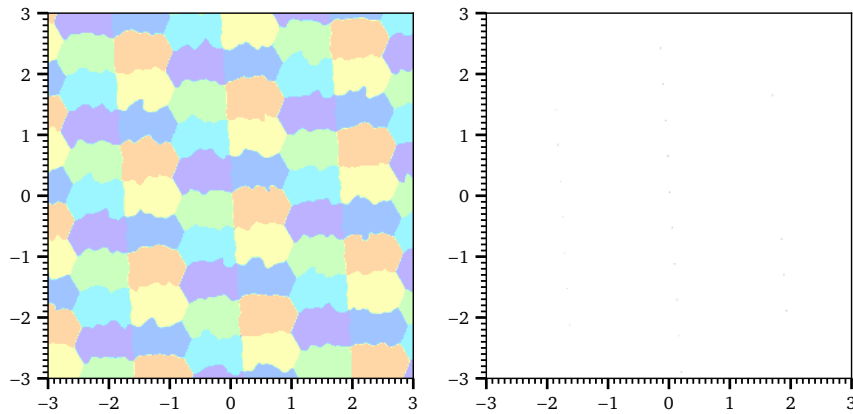


Figure 11: An almost-coloring for 6 colors, where only 0.04% of points need to be removed to avoid unit distances.

C. Details on variant 2: Avoiding different distances

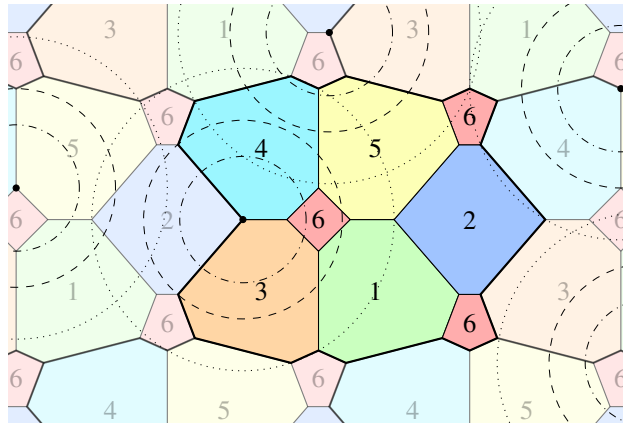


Figure 12: A 6-coloring of the plane where no red points appear at any distance between 0.418 and 0.657 while no other color has monochromatic unit-distance pairs. The dotted circles have unit distance radius, while the dashed circles have radius 0.657 and the dash-dotted circles have radius 0.418. Shown is the formalized version, which was inspired by the NN outputs, see also Figure 1.

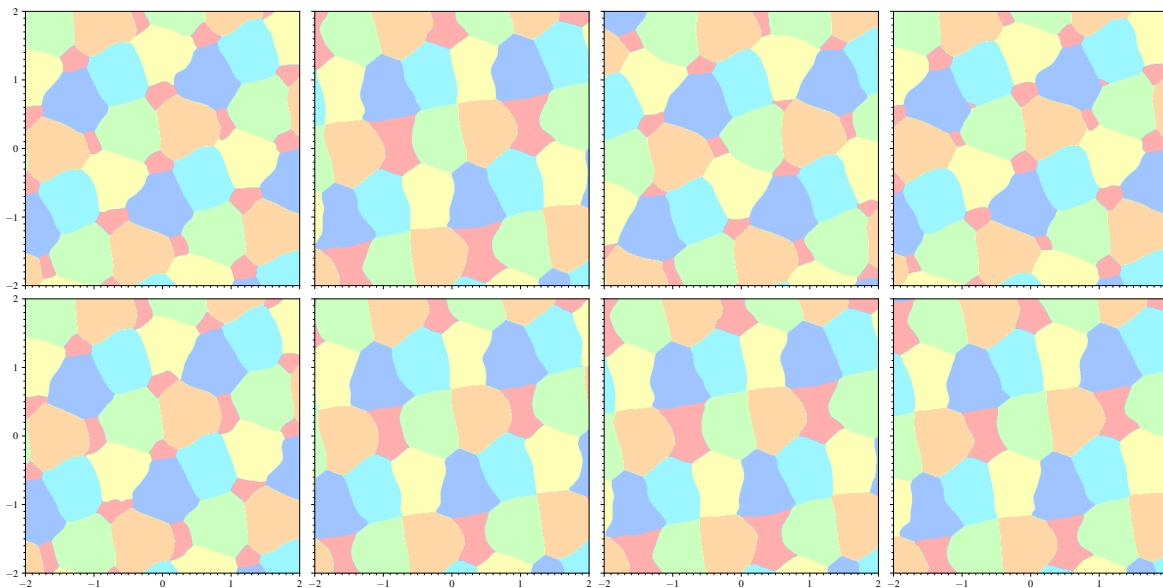


Figure 13: A more detailed view of the colorings generated by a single model for different values of the last distance. Upper row (from left to right): $d = 0.4$, $d = 0.6$, $d = 0.8$, $d = 1.0$. Lower row (from left to right): $d = 1.2$, $d = 1.4$, $d = 1.6$, $d = 1.8$.

The polychromatic number of the plane is the minimum number of colors needed such that no color realizes all distances in its monochromatic pairs. While known to be at most 6, finding a five-color solution would constitute a significant improvement. Our search focused on colorings of type (d_1, \dots, d_5) , where we set $d_1 = 1$ without loss of generality. Our approach sampled distances from $[0.2, 2.2]$ and included them directly in the domain of the NN. Rather than performing an expensive grid search over the four remaining distances, we employed first- and second-order optimization methods to find optimal values after training. This optimization led to our best result with distances $d_1 = 1$, $d_2 \approx d_3 \approx 1$ and $d_4 \approx d_5 \approx 0.56$, achieving a minimal conflict rate of approximately 5% (see Figure 7). This suggests that the polychromatic number of the plane may indeed be six.

Note that when including the distances in the domain of the function of the coloring, we conceptually parametrize a whole

family of implicit neural representations. Instead of viewing this as a function of both coordinates and distances as in Equation (7), we can view it as a function-valued function (i.e., an operator):

$$G : \prod_{k=1}^c [d_k^{\min}, d_k^{\max}] \rightarrow \{g \mid g : \mathbb{R}^2 \rightarrow \Delta_c\}. \quad (9)$$

This perspective connects to the rapidly growing field of operator learning (Kovachki et al., 2024). DeepONets (Lu et al., 2021) are particularly suitable architectures for such mappings, and have proven effective in the numerical treatment of differential equations (Wang et al., 2021; Mundinger et al., 2024b).

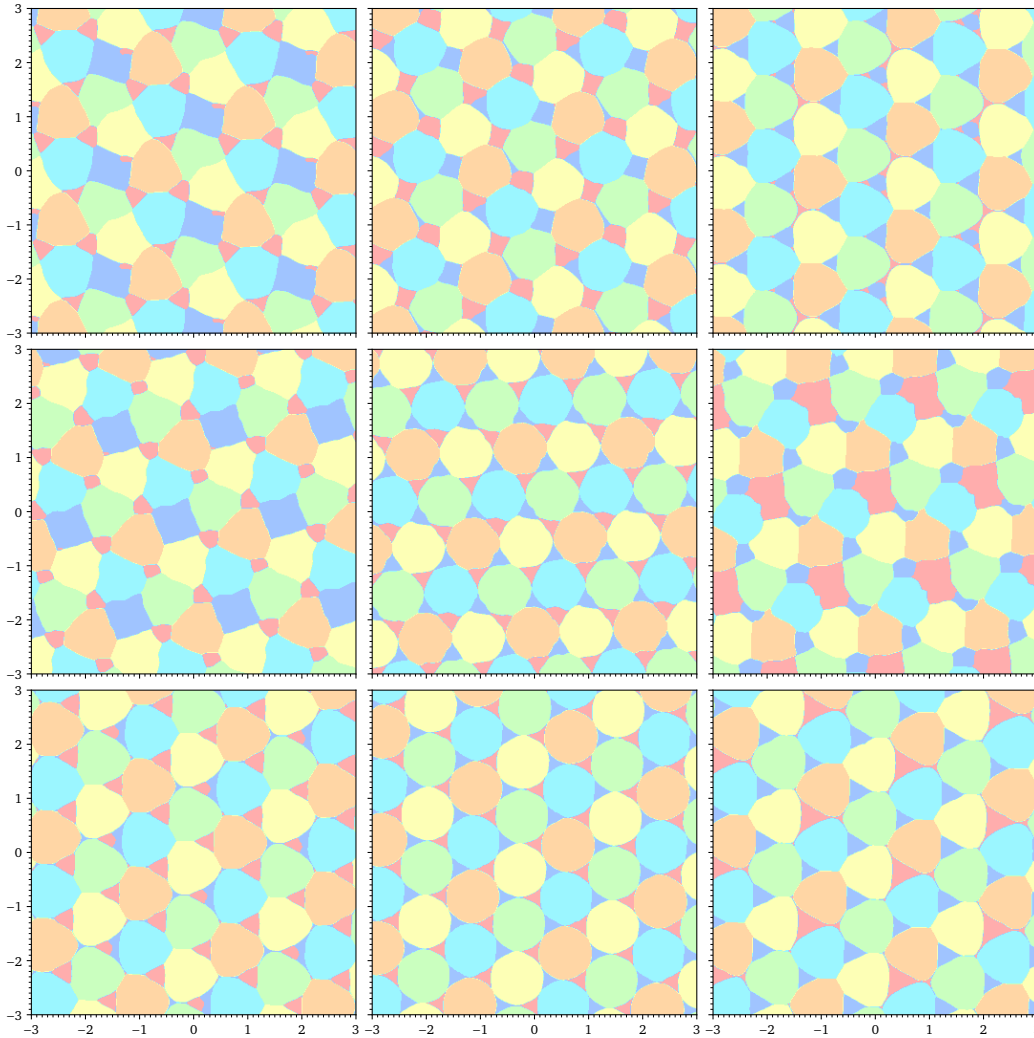


Figure 14: Three different distance configurations generated by the same model: $(d_1, d_2) = (1, 0.4)$ (left), $(0.5, 0.5)$ (middle), and $(0.6, 1.0)$ (right). The bottom two rows show patterns similar to Stechkin’s construction at $(0.5, 0.5)$, while the outer columns reveal patterns that led to our formalized constructions.

D. Details on Variant 3: Coloring three-dimensional space

Visualizing and thus also interpreting and formalizing a three-dimensional coloring is much more challenging than in the two dimensional case. To better understand the structure of colorings, we extracted polygons from the NN output and explored them in interactive plots. One of these colorings is shown in Figure 15.

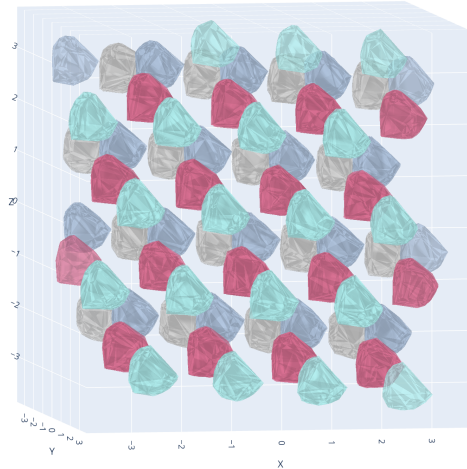


Figure 15: A three-dimensional coloring found by our approach. We only show four out of the fourteen colors.

E. Details on Variant 4: Avoiding triangles

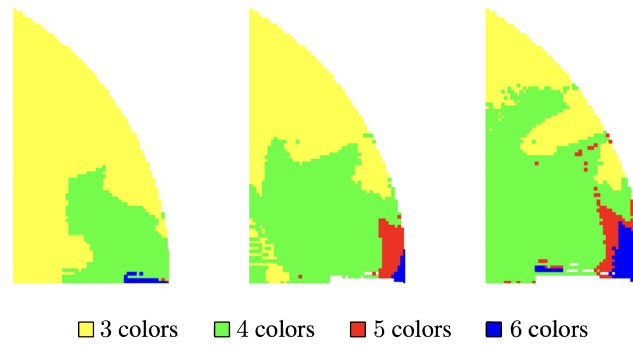


Figure 16: Numerical results showing the achievable color bounds when avoiding monochromatic triangles. We trained thousands of networks on different sub-areas of the above region and say that a point can be achieved with three, four, five, or six colors if the top 3% of runs for that point reported that less than 1% (left), 0.1% (middle), and 0.01% (right) of sampled triangles were monochromatic in the argmax coloring derived from the trained NNs.

F. Different p-norms

Our approach extends to different norms in \mathbb{R}^n . The loss function remains the same, while the respective ball $B_1(x)$ is replaced by the L_p -ball $B_p(x) = \{y \in \mathbb{R}^n \mid \|x - y\|_p \leq 1\}$. To generate samples from the L_p -ball, we use the probabilistic method proposed by Barthe et al. (2005). The cases $p = 1$ and $p = \infty$ in \mathbb{R}^2 are relatively straightforward to derive, as there exist colorings using four colors by arranging the balls in a regular grid. However, in particular the case $p = 1$ produces visually interesting results, as not only the trivial constructions are found but variations thereof, see Figure 17.

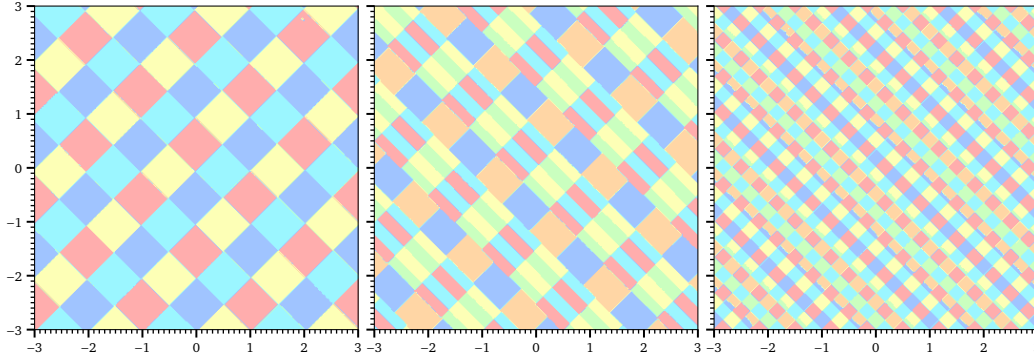


Figure 17: Colorings found for the L^1 norm. Left: The trivial grid coloring. Middle and right: Colorings which utilize the degrees of freedom present in the coloring.